

ARTICLE

An MHC-restricted antibody-based chimeric antigen receptor requires TCR-like affinity to maintain antigen specificity

Marcela V Maus^{1,2}, Jason Plotkin¹, Gopinadh Jakka⁵, Guillaume Stewart-Jones³, Isabelle Rivière¹, Taha Merghoub⁴, Jedd Wolchok⁴, Christopher Renner^{5,6} and Michel Sadelain^{1,7}

Chimeric antigen receptors (CARs) are synthetic receptors that usually redirect T cells to surface antigens independent of human leukocyte antigen (HLA). Here, we investigated a T cell receptor-like CAR based on an antibody that recognizes HLA-A*0201 presenting a peptide epitope derived from the cancer-testis antigen NY-ESO-1. We hypothesized that this CAR would efficiently redirect transduced T cells in an HLA-restricted, antigen-specific manner. However, we found that despite the specificity of the soluble Fab, the same antibody in the form of a CAR caused moderate lysis of HLA-A2 expressing targets independent of antigen owing to T cell avidity. We hypothesized that lowering the affinity of the CAR for HLA-A2 would improve its specificity. We undertook a rational approach of mutating residues that, in the crystal structure, were predicted to stabilize binding to HLA-A2. We found that one mutation (DN) lowered the affinity of the Fab to T cell receptor-range and restored the epitope specificity of the CAR. DN CART cells lysed native tumor targets *in vitro*, and, in a xenogeneic mouse model implanted with two human melanoma lines (A2+/NYESO+ and A2+/NYESO−), DN CART cells specifically migrated to, and delayed progression of, only the HLA-A2+/NY-ESO-1+ melanoma. Thus, although maintaining MHC-restricted antigen specificity required T cell receptor-like affinity that decreased potency, there is exciting potential for CARs to expand their repertoire to include a broad range of intracellular antigens.

Molecular Therapy — Oncolytics (2016) **3**, 16023; doi:10.1038/mto.2016.23; published online 16 November 2016

INTRODUCTION

Chimeric antigen receptors (CARs) are high-affinity ligand or single-chain variable fragment (scFv)-based receptors used to redirect T cells to recognize and lyse tumor cell targets. CD19-specific CAR T cells are emerging as a powerful clinical therapy,^{1,2} showing impressive outcomes in nonHodgkin lymphoma,³ chronic lymphocytic leukemia,⁴ and acute lymphoblastic leukemia.⁵

CARs are generally limited to native surface antigen targets.^{6,7} However, most of the known “high-priority” tumor antigens ranked by a National Cancer Institute panel,⁸ which includes universal tumor antigens and cancer-testis antigens, and most neoantigens, are intracellular proteins and are thus only subject to immune surveillance as cell surface peptides borne by MHC molecules. Expanding the repertoire of CARs to target intracellular antigens would open new avenues for cancer immunotherapy.

The T cell receptor (TCR) is the natural biologic receptor employed by the immune system for surveillance of cytoplasmic antigens. TCRs are typically low-affinity receptors (micromolar kD) that bind to peptide epitopes in the context of host MHC molecules. Several groups have explored retroviral transduction of native TCRs with the goal of redirecting T cells to intracellular antigens. However, these

transduced T cells have the potential to express four different T cell receptors (native-alpha/beta, transduced alpha/beta, and native/transduced heterodimers), which is problematic for two crucial reasons: (i) the native/transduced heterodimers have unknown specificity and potential autoimmune consequences,^{9,10} and (ii) there is dilution of the signal transduction apparatus, since the availability of CD3 complex molecules is limiting. Nevertheless, this approach has been applied in early clinical studies without mispairing-related adverse events.^{11,12} In an effort to resolve the potential mispairing issues, some investigators have also designed single-chain TCRs.¹³

Immunoglobulin structures share structural homology with TCRs and may mimic TCR recognition of HLA/peptide complexes.¹⁴ CARs incorporating such recognition elements would be advantageous in that they do not directly compete with the native TCR, and would further provide, in the case of second generation CARs, supportive costimulation to the transduced T cells.¹⁵ Phage display libraries have enabled the rapid isolation of human Fab fragments highly specific to peptide/MHC molecules.¹⁶ In early attempts, these types of antibodies were found to derive most of their affinity from binding to the MHC alpha helix, in a conformation quite different from the binding footprint of TCRs.¹⁷ More recently, a high-affinity Fab

¹Center for Cell Engineering, Memorial Sloan Kettering Cancer Center, New York, New York, USA; ²Current address: Cellular Immunotherapy Program, Massachusetts General Hospital, Cancer Center, Harvard Medical School, Boston, Massachusetts, USA; ³Division of Structural Biology, Wellcome Trust Centre for Human Genetics, University of Oxford, Oxford, UK; ⁴Ludwig Center for Cancer Immunotherapy, Swim Across America Laboratory, MSKCC, New York, New York, USA; ⁵Department of Oncology, University Hospital Zurich, Zurich, Switzerland; ⁶Department of Oncology, University Hospital Basel, Basel, Switzerland; ⁷Weill-Cornell Medical College, New York, New York, USA. Correspondence: M Sadelain (m-sadelain@ski.mskcc.org)

Received 13 April 2016; accepted 23 August 2016

restricted to HLA-A2/NY-ESO-1₁₅₇₋₁₆₅ has been generated (3M4E5) and affinity-matured by shifting the binding affinity from the MHC alpha-helix to the peptide (T1). Crystal structure analysis of these complexes confirmed a binding conformation that was nearly superimposable with the footprint of a TCR specific to the same MHC/antigen complex.¹⁸

Here, we have developed a novel TCR-like antibody into a CAR based on the scFv of a high-affinity antibody (T1) that recognizes HLA-A*0201 in combination with a peptide epitope derived from NY-ESO-1, a cancer testis antigen that is expressed in the cytoplasm in a wide variety of tumors but is not expressed in normal somatic cells.¹⁹ We hypothesized that transduction of T cells with this CAR would efficiently redirect T cells in an HLA-restricted, antigen-specific manner. We have found that, despite the exquisite peptide-specificity of the soluble antibody, the same Fab in the form of a cell-bound antigen receptor lost its epitope specificity. We further found that a targeted mutation to decrease the binding of the Fab to HLA-A2 improved CAR specificity. The affinity of the mutated antibody was in the range of naturally occurring TCRs (micromolar).

RESULTS

High-affinity MHC-restricted CARs do not maintain the specificity, evident in the soluble antibody form

The T1 Fab we used had undergone rational affinity maturation of a parental Fab that was generated by phage display. The T1 antibody displayed high specificity for HLA-A2/NY-ESO-1₁₅₇₋₁₆₅ by BIAcore and enzyme-linked immunosorbent assay (ELISA) assays.¹⁸ The T1 Fab structure was also determined to bind the NY-ESO-1₁₅₇₋₁₆₅/HLA-A*0201 complex in a very similar fashion to a native TCR specific for the same MHC/peptide antigen.¹⁸ We constructed a second-generation CAR based on the scFv of the T1 Fab. The scFv of T1 was cloned into the backbone of the CD28-CD3 ζ bi-cistronic γ -retroviral vector,²⁰ which includes an IRES-green fluorescent protein (GFP) sequence to facilitate analysis of transduced cells (Figure 1a).

As with other CARs, primary human T cells were very efficiently transduced with the T1-28z CAR, as measured by GFP expression (42%) and surface staining with A2/NY-ESO pentamers (38.8%) (Figure 1b). T1-28z CAR T cells were tested for *in vitro* cytotoxicity against the HLA-A2+ TAP-deficient cell line T2, pulsed with 10 μ g/ml of either cognate peptide or the irrelevant HLA-A2 restricted epitope of influenza matrix protein (flu, GILGFVFTL). Although the T1-28z CAR-T cells efficiently lysed NY-ESO-1 pulsed T2 cells even at low effector:target (E:T) ratios, we noted a decrease in specificity of lysis at higher E:T ratios (Figure 1c). Next, we tested a panel of native melanoma tumor cell lines, including SK-Mel-37 (HLA A2+, NY-ESO1+), SK-Mel-23 (HLA A2+, NY-ESO1-), and SK-Mel-52 (HLA A2-, NY-ESO+). We again observed HLA-A2- restricted but NY-ESO-1-independent cytotoxic activity of the T1-28z CAR-T at high E:T ratios. Although it is difficult to directly correlate chromium release *in vitro* data to *in vivo* efficacy or specificity, we remained concerned about the high cytotoxic activity toward HLA A2+ targets independent of NY-ESO-1 expression. A possibly related phenomenon is known to occur with very high affinity TCRs.²¹⁻²⁵ We hypothesized that despite the specificity of the high affinity T1 antibody, when the same antigen-binding region in the form of a CAR was subject to antigen-induced receptor clustering (T cell avidity), there was loss of specificity due to excessive CAR binding to HLA. To decrease the affinity of the T1 CAR without losing epitope specificity, we undertook a rational approach to decrease binding of the scFv specifically to the HLA-A2 alpha helix.

Directed mutations based on the crystal structure of the T1 scFv specifically reduce binding to HLA-A2

Based on the crystal structure of the T1 Fab binding to HLA-A2 presenting NY-ESO-1₁₅₇₋₁₆₅, the amino acid residues in the light chain of the T1 scFv at positions D53 and Y34 were predicted to be essential candidates in stabilizing the binding of the T1 scFv to the HLA A2 alpha helix (Figure 2a). Breaking the salt bridge at D53 was predicted to have a significant impact on binding. Mutating this residue to an asparagine (N) would preserve the steric properties but reduce the salt bridge between the aspartic acid (D53) residue and the basic arginine residue (R65) of MHC. The Y34 ring forms part of an aromatic cluster, while the OH group of tyrosine (Y) hydrogen-bonds to the carbonyl group (CO) at MHC R65. Mutation of this Y34 to a phenylalanine (F) would preserve the aromatic cluster but not maintain the hydrogen bonding. Using a panel of linkers in the T1-28z retroviral construct sequence, we made the D53N and Y34F mutations alone and in combination, expecting to break one salt bridge and decrease hydrogen bonding while preserving the steric properties important for the stability of the complex. A mutation in the heavy chain of the T1 scFv, at the K65 position, was predicted to have a smaller impact on affinity because it is largely solvent-exposed. This residue was mutated to T to retain some of the Ca/Cb stalk that is packed against the CDR2 Y60 in the heavy chain. This mutation was evaluated separately for technical ease of generating the mutants.

T cells transduced with the T1-28z CAR incorporating the light chain mutations DN, YF, or both (DNYF) were evaluated for pentamer binding by fluorescence-activated cell sorting (FACS) (Figure 2b) and for cytotoxicity against peptide-pulsed T2 cells (Figure 2c). Based on the mean fluorescence intensity of pentamer binding under the same conditions, it was clear that the DN mutation had a significant impact in lowering the affinity of the T1 CAR (Figure 2b). The YF mutant had no significant impact, while the DNYF mutant had a moderate effect on pentamer binding. *In vitro* cytotoxicity assays against T2 cells pulsed with either NY-ESO-1 or flu peptide revealed distinct separation of the curves with the DN-transduced T cells, with preserved lysis of antigen-bearing targets. The YF mutation had no discernable effect in this *in vitro* functional assay. The heavy chain mutation K65T alone had no significant effect on pentamer binding or cytotoxicity, and did not appear to have additive effect when combined with the DN mutation (DNKT) (data not shown). Based on these data, the DN mutant version of the T1/28z CAR (DN/28z) became our leading candidate. The K65T mutation had negligible impact compared with the DN mutation (Supplementary Figure S1).

BIAcore measurement of the DN mutation in T1 reveals significant decrease in affinity

To measure the affinity of the DN mutant directly, we generated Fabs with the DN mutation and performed surface plasma resonance (BIAcore). Two versions of the NY-ESO-1 peptide were examined (9C and 9V), because the naturally occurring cysteine (C) at the ninth position in the peptide epitope can sometimes form disulfide bonds that interfere with the binding measurements of interest. The binding of DN Fab to the 9C and 9V peptides was measured over a range of five different concentrations; the kD was calculated at 672 nmol/l (9C) and 715 nmol/l (9V) (Figure 3). The kD of the parental T1 Fab was 2 nmol/l (9C) – 4 nmol/l (9V).¹⁸ Neither Fab bound to flu peptide at all (flat line, data not shown). In a study comparing BIAcore affinities of antiviral TCRs (A2 Tax, A24 EBV, B27 flu, B8 EBNA, and A2 flu) to the tumor-associated antigen TCRs (A2 mel, A2 gp100, and A2 telomerase), the average kD of a viral antigen TCR was 9 ± 7 μ mol/l,

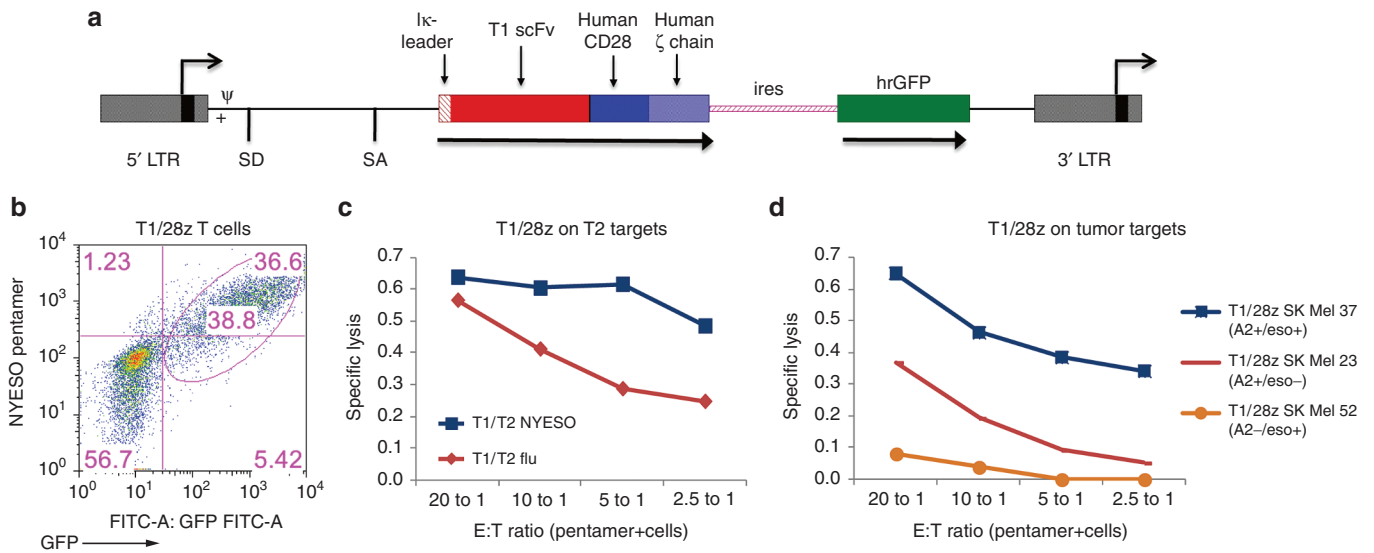


Figure 1 T1/28z CAR construct. (a) SFG vector indicating LTRs, packaging signal (ψ), splice donor and splice acceptor sites, leader sequence, single-chain variable fragment of the T1 (HLA-A2/NYESO1-specific) antibody fused to human CD28 and human CD3zeta signaling domains. The ires-GFP domain is 3'. (b) Primary human T cells 5 days after transduction with T1/28z retroviral vector, stained with HLA-A2/NYESO pentamer. Cells are gated on FSC/SSC only. Chromium release cytotoxicity assay using T1/28z-transduced T cells as effectors against (c) T2 cells pulsed with 10 μ g/ml of either NYESO1 or flu peptide. E:T ratios normalized to pentamer+ cells or (d) human melanoma lines SK Mel 37, SK Mel 23, or SK Mel 52. GFP, green fluorescent protein; E:T, effector:target.

whereas the average kD of Class I-restricted tumor-associated antigen-specific TCRs was $21 \pm 12 \mu\text{mol/l}$.²⁶ Specifically, the 1G4 HLA-A2/NY-ESO-1 specific TCR is in the 6–13 $\mu\text{mol/l}$ range, which is slightly higher than the published BIAcore studies of the affinity of the JM22 TCR specific for HLA-A2/flu.²⁷ Thus, the antigen-recognition region of the DN Fab has an affinity that is significantly lower than a high-affinity antibody, but slightly higher than naturally occurring TCRs specific for viral antigens (Table 1).

The DN mutation restores specificity to antigen in transduced T cells

Next, we tested the parental T1-28z CAR and DN-28z CAR T cells for their ability to lyse target cells in an antigen concentration-dependent manner. We found that T1-28z CAR T cells lysed NY-ESO-1-peptide pulsed T2 cells independent of peptide concentration (ranging from 0 to 10 $\mu\text{g/ml}$, Figure 4a), confirming the peptide-independent lysis observed at high E:T ratios previously. In contrast, DN-28z CAR T cells lysed NY-ESO-1-peptide pulsed T cells in a concentration-dependent fashion, indicating restored antigen specificity with the lower affinity receptor (Figure 4b). Because the potential clinical application of these A2/NY-ESO-1 CARs only applies to patients who have the HLA-A2 genotype, we also examined the growth of the T1 and D53N CARs when transduced into T cells from an individual with the HLA-A*0201 genotype. The CAR T cells were rested for a week after transduction and then stimulated *in vitro* with mouse-fibroblast-based artificial APCs²⁸ transduced with HLA-A*0201, β_2 -microglobulin, and full-length NY-ESO-1 (in addition to CD80, ICAM, and LFA3). We noted that T1-transduced T cells expanded less than DN-CAR T cells over 5 days, suggesting ongoing fratricide in the HLA-A2+ cultures (Figure 4c). Similarly, when HLA-A2+ T cells were stimulated with natural tumor HLA-A2+ NY-ESO-1+ tumor cells (multiple myeloma U266), or peptide-pulsed T2 cells, the proliferative response of T1-28z CART cells was impaired compared with CART cells transduced with DN-28z CARs. This effect was most pronounced at high levels of antigen expression (U266 and T2+NY-ESO-1) rather than lower levels of antigen expression

(SK Mel 37). Interestingly, this could not be solely explained by HLA expression levels (Supplementary Figure S2).

We attempted to test the safety of the T1-28 and DN-28z CAR T cells in HLA-A2 transgenic NSG (nonobese diabetic, SCID, gamma-chain knockout) mice,²⁹ hypothesizing that severe GvHD directed against HLA-A2 would develop in the T1-28z CART cell-treated mice. To avoid an allogeneic anti-HLA-A2 response, we used T cells from donors with the HLA-A*0201 genotype. Preliminarily, we found that the expression of HLA-A2 was several logs higher in the human donor T cells than in any of the NSG/A2 transgenic mouse blood cells or tissues (data not shown). Mice were injected with a single dose of either T1-28z or DN-28z CAR T cells, and sacrificed at pre-determined intervals for histopathologic analysis of organs that were most likely to be targets of an anti-HLA-A2 response (granulocytes, lungs, liver, and skin). None of the mice developed clinical signs of GvHD-type disease (skin ruffling, weight loss, or loss of fur) over 3 weeks, but they all developed hair loss at 6 weeks; this is typical for NSG mice injected with human T cells, and is thought to be mediated by a xenogeneic response of human T cells directed to mouse MHC molecules. At days 14 and 22, there were higher levels of T cell infiltration into the lungs and livers of mice that received the T1-28z-CAR-T compared with those that received either DN-28z-CAR-T or mock-transduced-T (Supplementary Figure S3), but both forms of CAR T cells resulted in greater lymphocyte infiltrate than untransduced T cells. T cell infiltrates were quantified on a 0–4 grading system developed by expert veterinary pathologists, but these assessments were more qualitative overall than strictly quantifiable (Supplementary Table S1). There was no effect on the white blood cell counts in the mice (data not shown). Interestingly, a greater effect was imparted on the persistence of the HLA-A2+ CD3+ GFP+ human T cells, which had a much higher level of HLA-A2 expression than the mouse tissues. Although all the mice were injected with the same number of CD3+ GFP+ T cells, the DN-28z CART cells achieved higher circulating levels of CD3+ T cells in the blood at day 15, again suggesting some degree of fratricide among the T1-28z-transduced HLA-A2+ donor T cells (Figure 4e). Taken together, these

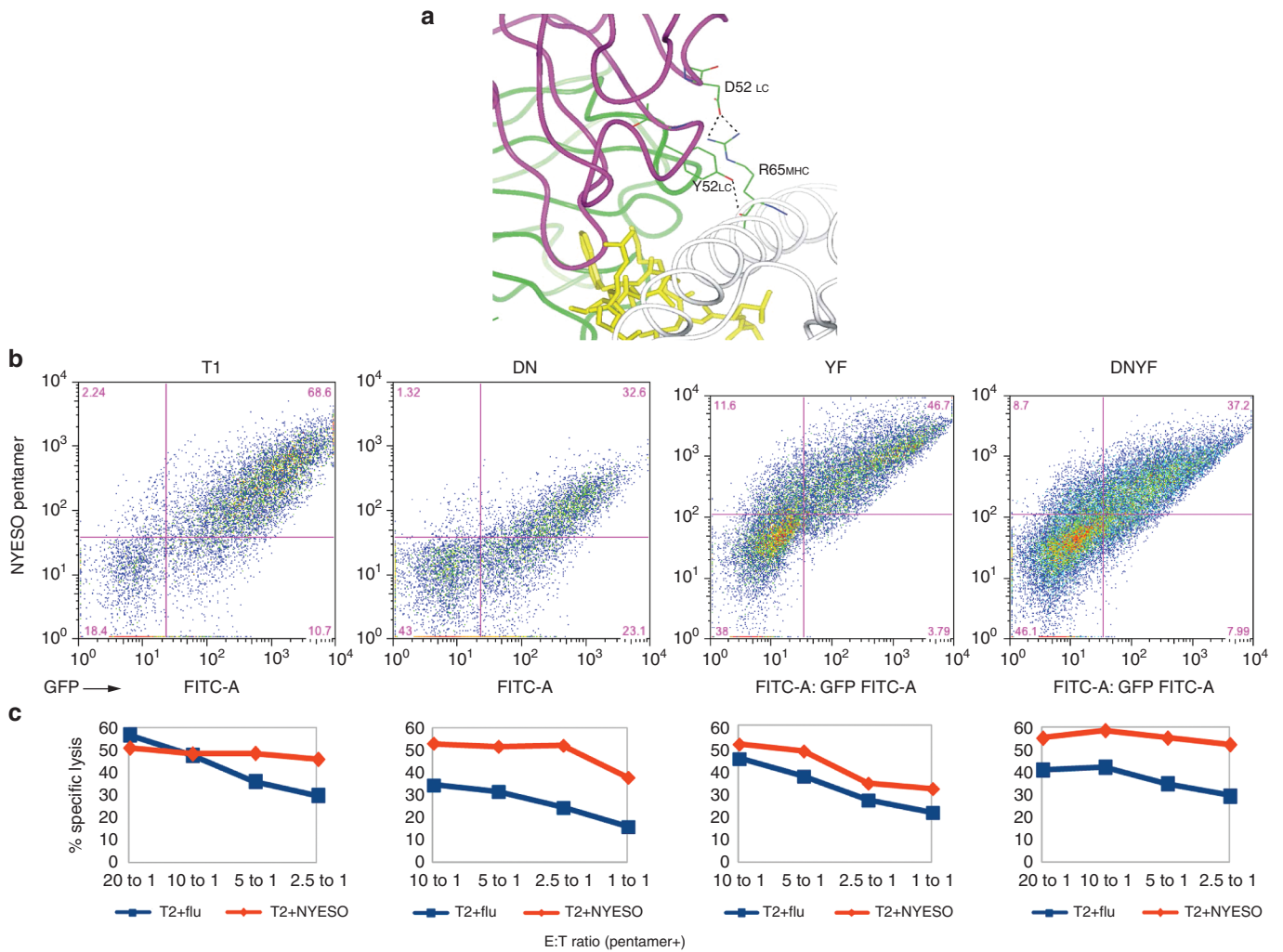


Figure 2 Rationally targeted mutations designed to decrease binding of T1 to HLA-A2/ NYESO1. **(a)** Crystal structure of T1 Fab binding HLA-A2/ NYESO1, with highlighting of targeted amino acids. **(b)** A2/NYSEO1 pentamer stains of primary human T cells 5 days after transduction with parental (T1), D53N mutant, Y34F, and DNYF mutations in the CAR. Fluorescence-activated cell sorting (FACS) plots are gated on FSC/SSC only. **(c)** Chromium release assays of corresponding CAR-transduced effectors against T2 cells pulsed with either flu or NYESO peptide as targets. Effector to target ratios are normalized to pentamer+ cells. CAR, Chimeric antigen receptor.

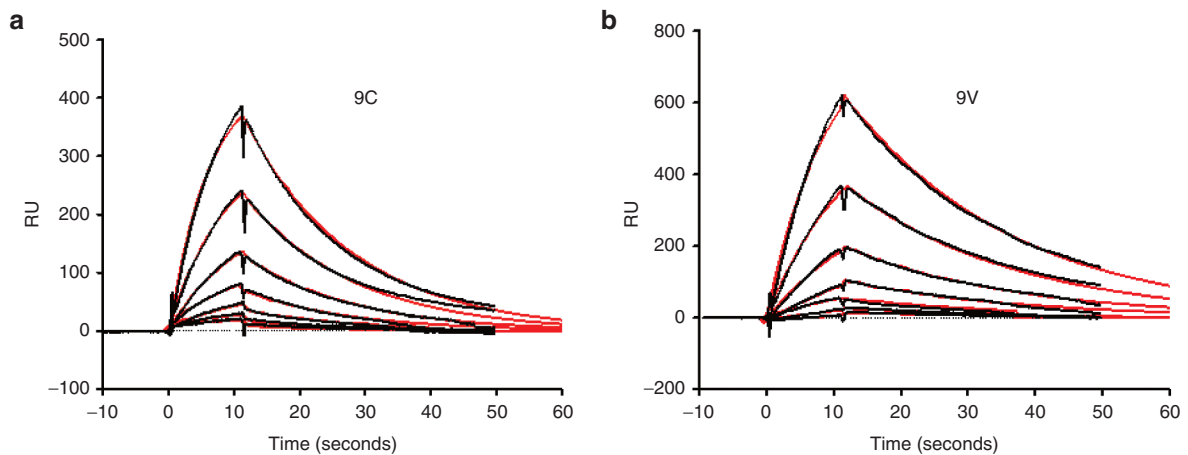


Figure 3 Direct measurement of affinity of the DN mutation in the Fab antibody by BIAcore. Sensograms of DN Fab run over a range of concentrations (18.5 nmol/l – 1187 nmol/l) of HLA-A2 presenting **(a)** native NYESO1 (SLLMWITQC) or **(b)** mutant C9V NYESO1 (SLLMWITQV) peptide, which avoids disulfide bonding. Data were fitted (red) in a BIAevaluation 3.0 following a simple 1:1 Langmuir binding model.

Table 1 Comparison of BIAcore affinities of select MHC-restricted antibody- and TCR-based receptors

Analyte	Peptide	K_{off} /mol/second	K_{off} /second	K_D (K_{off}/K_{on}), nmol/l	Reference
DN	SLLMWITQC; SLLMWITQV	90,100; 56,000	0.0606; 0.0401	672; 715	
T1	SLLMWITQC; SLLMWITQV	138,375; 249,000	0.000674; 0.000835	2; 4	Stewart-Jones PNAS (2009) ¹⁸
1G4 TCR	SLLMWITQC; SLLMWITQV	12,200; 11,800	0.17; 0.049	13,300; 5,700	Chen JEM (2005) ²⁷
JM22 TCR	GILGFVFTL; GILGFVFTL	18,000; 40,000	0.03; 0.2	1,000; 6,000	Cole JI 2007; Wilcox Immunity (1999)
FMC63 (aCD19)	Antibody; scFv			$1/4.2 \times 10^{-9}$; $1/2.3 \times 10^{-9}$ ($\sim 3 \times 10^8$)	Nicholson Mol Imm (1997)

scFv, single-chain variable fragment; TCR, T cell receptor.

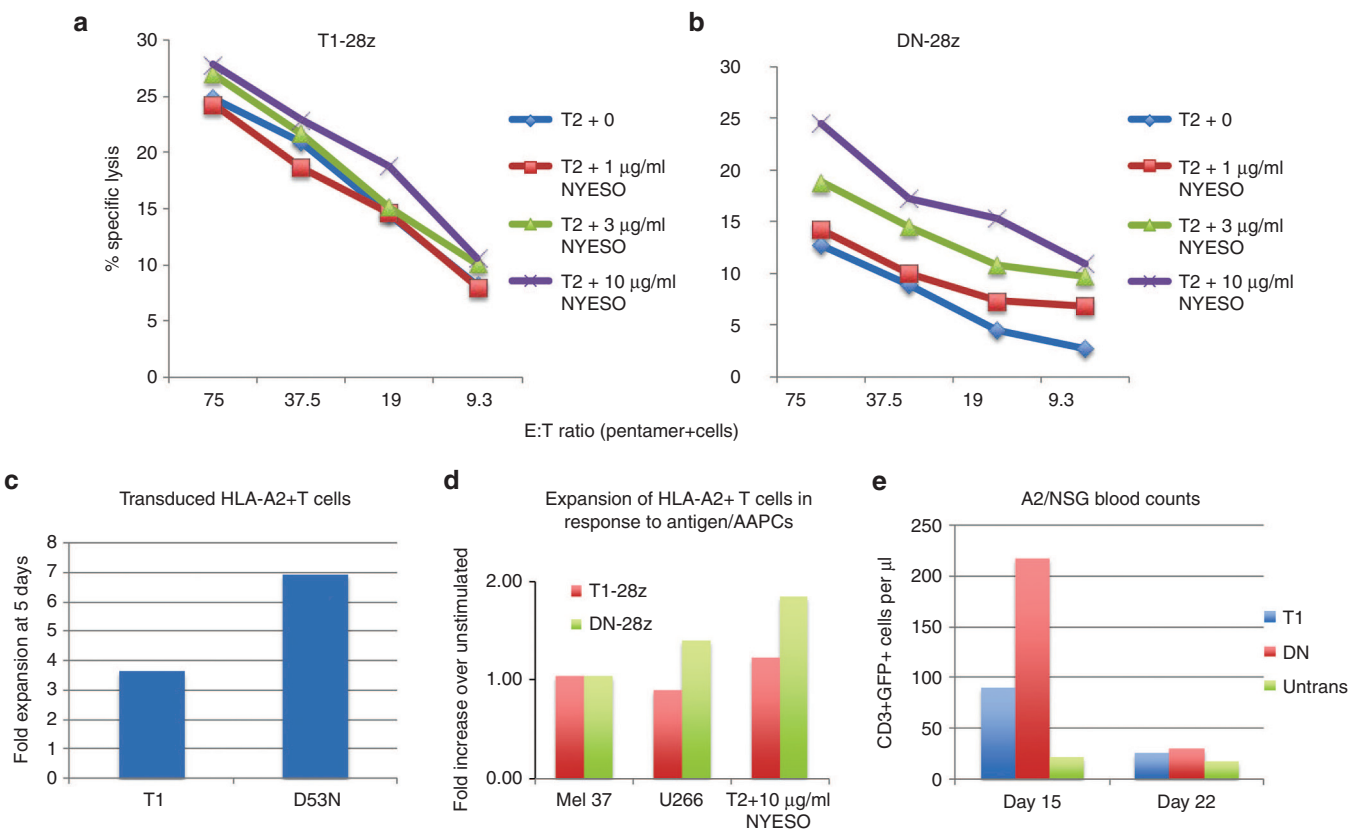


Figure 4 DN mutation restores epitope specificity of T1-antibody-based CAR-transduced T cells. Chromium release assays using (a) T1/28z CAR-transduced or (b) DN/28z CAR-transduced T cells as effectors against target T2 cells pulsed with titrating concentrations of NYESO1 peptide. (c) Expansion of T1/28z and DN/28z CAR-transduced T cells derived from an HLA-A2+ donor. T cells were rested for one week after transduction and then stimulated with artificial APCs. Growth of CD3+GFP+ cells was calculated as total number of lymphocytes \times frequency of CD3+GFP+ cells as determined by fluorescence-activated cell sorting (FACS) staining. (d) Expansion of HLA-A2+ T cells in response to antigen. Data are shown as fold-increase over unstimulated cells. Mel 37 is the SK-Mel 37 tumor cell line (HLA-A2+, NY-ESO-1+); U266 is the multiple myeloma cell line (also HLA-A2+, NY-ESO-1+). Proliferation was measured 4 days after restimulation. (e) Absolute number of CD3+GFP+ T cells per μ l of blood at two timepoints after injection of NSG-HLA-A2 transgenic mice with T1/28z-, DN/28z-, or untransduced HLA-A2+ T. CARs, Chimeric antigen receptors; GFP, green fluorescent protein.

data suggest that the DN mutation has a significant impact on specifically detargeting the HLA-A2 molecule.

DN-28z CART cells lyse tumor targets as effectively as T1-28z *in vitro*. Having improved the *in vitro* and *in vivo* "safety profile" of the T1 scFv with the D53N mutation, we turned our attention again to the efficacy of the lower affinity DN-28z CART T cells toward lysing native

tumor targets. T cells were transduced with the T1-28z or DN-28z CARs in preparation for the subsequent *in vitro* and *in vivo* studies. Here again we confirmed the lower affinity of the DN mutant by mean fluorescence intensity of pentamer staining; T1-28z-transduced T cells had an MFI of 596, while the DN-28z-transduced T cells had an mean fluorescence intensity of 170, after gating on GFP+ cells (Figure 5a,b). About 1 week after transduction, DN-28z CAR T cells

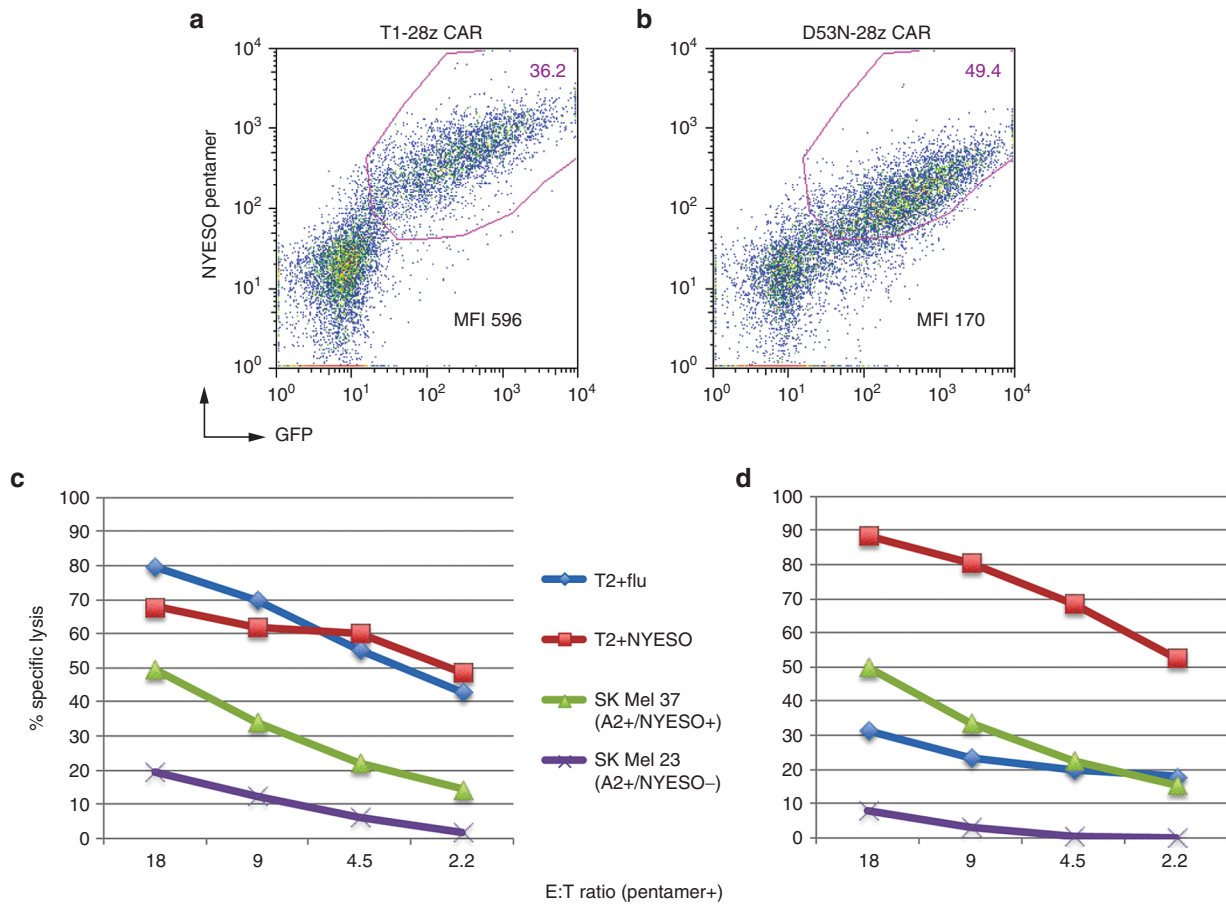


Figure 5 Similar efficacy of T1/28z and DN/28z CAR-transduced T cells. A2/NYESO1 pentamer stains of T cells transduced with (a) T1/28z or (b) DN/28z CAR. MFI shown is mean fluorescence intensity of GFP+ cells. Plots shown are gated only on fsc/ssc. Chromium release assays of (c) T1/28z or (d) DN/28z CAR-transduced T cells against peptide-pulsed T2 cells and against native tumor targets (melanoma cell lines SK-Mel-37 and SK-Mel-23). DN/28z T cell culture was diluted with untransduced T cells to equalize the frequency of pentamer+ cells with the T1/28z T cell culture. Effector: target ratios are normalized to pentamer+ cells. CARs, Chimeric antigen receptors.

were able to lyse NY-ESO-1-peptide pulsed T2 cells and native tumor targets (SK-Mel-37, HLA-A2+/NY-ESO-1+) as well as the T1-28z CAR T cells. Lysis of flu-pulsed T2 targets and HLA-A2+ NYESO1- targets (SK Mel 23), however, was much reduced (Figure 5c,d).

A2/NYESO-CAR (DN)-transduced T cells specifically infiltrate and delay progression of an NY-ESO-1 expressing tumor *in vivo*
 Next, we set up a xenogeneic mouse model utilizing the NSG strain that permits long- term engraftment of human cells.³⁰ To address whether human T cells transduced with the DN-28z CAR could specifically home to a NY-ESO1+ tumor, NSG mice were injected subcutaneously on day 0 with 3×10^6 SK-Mel-37 human melanoma cells on one flank and 3×10^6 SK-Mel-23 human melanoma cells on the other. DN-28z CAR T cells were infused at four different doses in each group of five mice. An intermediate dose of 2×10^6 19-28z CAR T cells (using the same vector backbone) was infused in a group of control mice. Tumors were measured until day 33. At the time of sacrifice, the tumors were excised and analyzed by immunohistochemistry for infiltration by human CD3+ T cells. All the subcutaneous tumor implants were noted to exhibit central necrosis, but in the mice injected with DN-28z-transduced T cells, the rim of SK-Mel-37 (NY-ESO-1 positive) tumors demonstrated infiltration by human CD3+ T cells (Figure 6a, c); the total number of T cells per mm² of tumor was dose-dependent (Figure 6a). In contrast, the SK-Mel-23 (HLA A2+/NYESO-negative) tumor in the same mice was not

infiltrated with T cells (Figure 6b,d). In mice that were injected with CD19 CAR-transduced T cells, there was no infiltration of human T cells into either tumor (data not shown).

In addition to infiltrating the NY-ESO-1+ tumors, DN28z CAR T cells were detectable in the peripheral blood and spleen of tumor-bearing mice past day 30 (Supplementary Figure S3). At the lowest dose of T cells, DN-28z CAR T cells were detected at a frequency of 5 cells per μ l of blood; at the highest dose, the frequency was more variable but ranged from 5 to 30 cells per μ l of blood. DN-28z CAR T cells were also detectable in the spleens at similar frequencies at all doses. No CD19-28z CAR T cells were detectable in blood or spleen past day 30, consistent with prior data indicating the need for continued antigen stimulation to maintain 28z-based CAR-transduced T cells.³¹

Compared with treatment with T cells transduced with the irrelevant 19-28z CAR, the DN-28z CAR T cells significantly delayed growth of only the NY-ESO-1+ tumor (SK-Mel-37). This was most clearly evident at the highest dose of DN-28z-CAR-T cells (Figure 6e,f). Unfortunately, disease-specific survival could not be measured in this model for two reasons: first, the NY-ESO-1-negative tumor (SK-Mel-23) was much more clinically aggressive, and was not impacted by the DN-28z CAR T cells, making the survival data from these bilateral-tumor experiments not evaluable. Second, the survival of NSG mice injected with human T cells is confounded by a xenogeneic graft-vs-host disease (GVHD) effect, which begins to clinically affect the mice 4–6 weeks after T cell infusion (data not shown and ref. 32). This model is not

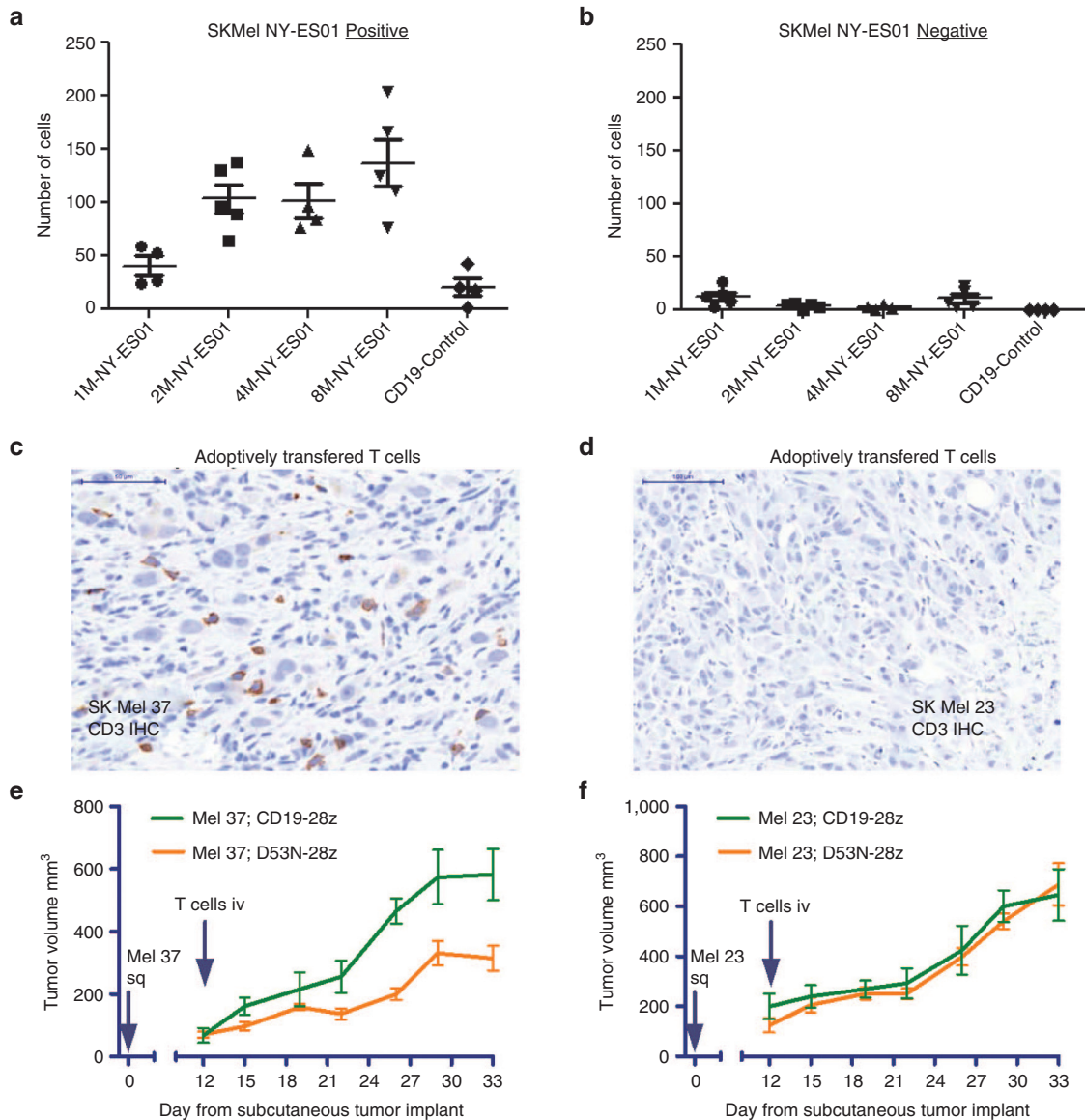


Figure 6 DN/28z CAR-T cells specifically traffic to and delay progression of an NY-ESO-1-positive melanoma tumor in a xenogeneic mouse model. Subcutaneous tumor implants of mice treated with escalating doses of DN/28z CAR-T cells (or CD19/28z CAR-T cells as a control) were harvested and stained for CD3 by immunohistochemistry. The number of CD3+ T cells infiltrating the (a) SK Mel 37 (NY-ESO-1 positive) and (b) SK Mel 23 (NY-ESO-1 negative) was quantified as cells per mm². Representative slides of the tumors from mice treated with 8×10^6 CAR-T cells are shown (c,d). The volume of each tumor (e,f) over time in mice treated with the 8×10^6 DN/28z CAR-T cells or control T cells is shown. Lines are plotted as mean \pm SEM of five mice for each group. CAR, Chimeric antigen receptor; SEM, standard error of mean.

aggressive enough to cause lethality in that time frame, and any possible survival data even with a single tumor implant would be confounded by the effect of this xenogeneic GVHD.

DISCUSSION

We sought to extend the applicability of antibody-based CARs to intracellular antigens because this approach has the potential to open access to an unlimited repertoire of monoclonal antibodies, while circumventing the problem of mispairing of transduced receptors with the endogenous TCR α/β chains, and extending the benefits of costimulatory engineering of CARs to HLA-peptide targeting. We found that maintaining the specificity of a CAR-based receptor for an intracellular antigen to be significantly more complex than targeting other cell surface molecules. Specifically, we found that the affinity of the antibody directed to an intracellular

antigen and binding to HLA need to be carefully evaluated upon conversion to a CAR and expression in T cells. Minimal binding to HLA may cause loss of CAR specificity, likely owing to the increased avidity resulting from CAR clustering at the cell surface.

Currently, there are three examples of CARs based on antibodies that bind HLA/peptide that appear to have high specificity and cytotoxicity *in vitro* and in xenogeneic mouse models: one is specific to HLA/EBNA3C and resulted in high cytotoxicity when introduced into NK cells³³; another is specific for HLA-A2/gp100 and was found to suppress melanoma progression in a xenograft model when introduced as a CAR into human T cells,³⁴ and one is specific for HLA-A2/WT1 and appears to have high specificity and cytotoxicity *in vitro* and in xenogeneic mouse models of leukemia.³⁵

Our study and others, however, have further scrutinized the “background activity” of engineered T cells, not just of the scFv. In

one such study, an HLA-A2/WT1-specific CAR based on a single-chain variable fragment showed decreased cytotoxicity and poor specificity compared with a low-affinity TCR specific to the same antigen, despite the higher affinity of the scFv.³⁶ In another study, antibodies specific to MHC/peptide complexes were isolated after immunization of HLA-A2 transgenic mice, and their variable fragments used to design CARs, but these required >100-fold higher antigen density to exert cytotoxicity compared with a cognate T cell clone bearing a natural TCR.³⁷

The optimal affinity of an antigen receptor that is MHC-restricted and specific to a peptide epitope has not been definitively defined. TCRs target these complexes efficiently³⁸ but generally with low binding affinity.³⁹ The range of affinities of naturally-occurring TCRs, even for viral epitopes, is in the micromolar range.⁴⁰ Indeed, engineered high affinity TCRs often result in decreased specificity.^{21–23} Furthermore, there is evidence that for TCRs, there is a maximum affinity threshold that limits T cell function ($kD \sim <5 \mu\text{mol/l}$), beyond which higher affinities do not increase clustering, signaling, lysis or growth. CAR-based receptors that are directed to surface molecules typically have high affinities (in the low nmol/l range), but affinity studies are not required to optimize specificity. On the other hand, very low affinity CARs specific for cell surface proteins may display poor efficacy, independent of epitope location on the target antigen.⁴¹

The minimal affinity of the antigen binding domain of a CAR required to trigger effective signaling has not yet been determined. We found that the low-affinity DN-28z CAR was sufficient to trigger specific lysis of peptide-pulsed targets, and natural HLA-A2-bearing, NY-ESO-1 expressing tumor cells (SK-Mel-37). Interestingly, the decreased HLA binding of the DN CAR relative to T1 also resulted in decreased T cell fratricidal activity. Although our SK-Mel-37 xenogeneic mouse model was not optimized, we were disappointed to find that the tumors were not eradicated despite infiltration of the DN CAR T cells and their persistence in the blood for over 1 month. This is a new xenogeneic model, and it is not clear how sensitive it is to adoptive cell therapies. Nevertheless, we interpret this outcome to reflect insufficient signal strength provided by the low-affinity CAR to effectively eliminate macroscopic tumor deposits. This finding points to the contradictory affinity requirements to achieve T cell potency while maintaining specificity.

The signal strength of physiological TCRs is augmented by engagement of additional molecules. Thus, the TCR/MHC interaction is stabilized by MHC binding to CD8 and consequent signaling through *Ick*; the engagement of additional costimulatory receptors, including B7 and TNF receptor family members, trigger separate signaling cascades that influence the function of the responding T cell. The second-generation CAR described here included a CD28 signaling domain, which may be suboptimal in the setting of very low affinity such as with the DN CAR. We previously demonstrated that the *in vivo* effects of low-activity CARs can be rescued through T-cell encoded costimulatory ligand expression^{42,43} or the use of chimeric costimulatory receptors.^{44,45} These two approaches may be valuable to enable the use of HLA-restricted CARs to target intracellular proteins.

MATERIALS AND METHODS

Cell lines and cell culture

Blood samples were collected from donors after giving written informed consent. High-resolution HLA-typing was previously known in HLA-A2+ donors, and only confirmed by antibody staining for HLA-A2. Normal human peripheral blood mononuclear cells were prepared from healthy donors by ficoll gradient centrifugation. T2 cells and the melanoma tumor cell lines SK-Mel-23 and SK-Mel-37 were provided by the Ludwig Center for

Immunotherapy at Memorial Sloan-Kettering Cancer Center. For transduction with CARs, peripheral blood mononuclear cells were stimulated with PHA at 2 $\mu\text{g/ml}$ on day 0 and transduced with viral supernatants on day 2. Recombinant hIL-2 was added at 50 IU/ml starting on day 2 and replenished every 2–3 days during *in vitro* culture. T cells were cultured in Roswell Park Memorial Institute (RPMI) supplemented with 10% fetal bovine serum, glutamine, and antibiotics. To assess T cell growth, transduced T cells were cultured at a 10:1 ratio with artificial APCs generated in our laboratory and previously described²⁸; these were additionally transduced with full-length NY-ESO-1 protein using a retroviral vector. Expression was confirmed by intracellular staining with the E978 antibody (Santa Cruz Biotechnology, Santa Cruz, CA).

Generation of retroviral T1-CAR constructs and mutants

The single-chain variable sequence (heavy chain—GSG linker—light chain) for the parental T1 construct¹⁸ was cloned into the SFG-28z-ires-GFP vector previously generated in our laboratory.^{20,46} The D53N, Y34F, and DNYF mutants were generated by a series of linkers and standard molecular biology techniques. All constructs were verified by sequencing (Genewiz). The RD30-HEK293 packaging line was transfected with the construct of SFG DNA, and viral supernatants were collected at days 2 and 3; these supernatants were used to make stable Galv9-HEK293 producer cells, from which viral supernatants were collected from confluent dishes to transduce T cells. Packaging cell lines were cultured in Dulbecco's modified Eagle's medium (DMEM) supplemented with 10% fetal bovine serum, glutamine, and antibiotics.

Staining and flow cytometry

Transduced T cells were analyzed for GFP expression and expression of cell surface molecules by standard staining and flow cytometry techniques. HLA-A2/NY-ESO1 pentamers were purchased from Proimmune (Oxford, UK). Antibodies to CD3 and HLA-A2 were purchased from BD Biosciences (San Jose, CA). Blood samples of 50 μl from mice were ACK-lysed and stained for 20 minutes at 4 °C with CD3 antibody; T cells were quantified with Count Bright counting beads (Invitrogen, Grand Island, NY).

Chromium release assays

In vitro cytotoxicity assays were performed according to standard techniques. Briefly, target cells were labeled with ⁵¹Cr (sodium chromate) for 90 minutes, then washed and co incubated for 4–6 hours in 96-well round bottom plates in triplicate with diluting ratios of effector T cells. Supernatants were harvested, transferred to Luma Plates (Perkin-Elmer, Shelton, CT) and acquired on a Perkin Elmer Top Count. Percent specific lysis was calculated with the formula $(x - \text{spontaneous}) / (\text{maximum} - \text{spontaneous})$. Peptide pulsing was performed where indicated either overnight or simultaneous with chromium labeling. HLA-A2 restricted influenza matrix protein (Flu, GILGFVFTL) and NY-ESO-1_{157–165} (SLLMWITQC) peptides were purchased from Proimmune.

Surface plasmon resonance measurements of affinity

SPR studies were performed using a Biacore 3000 (Biacore AB) as previously described.¹⁸ HLA-A*0201-SLLMWITQC and HLA-A*0201-SLLMWITQV were enzymatically biotinylated by BirA enzyme on the C-terminal biotinylation site and immobilized to CM5 sensor chips via covalently coupled streptavidin. Sensograms were measured over seven concentrations of D53N Fab. Kinetic constants were derived using the curve-fitting facility of the BIAevaluation program (version 3.0; Biacore AB) and rate equations derived from the simple 1:1 Langmuir binding model.

Mouse studies

NSG (stock # 005557-NOD.Cg-Prkdcscid Il2rgtm1Wjl/SzJ) and HLA-A2-transgenic NSG (stock#009617-NOD.Cg-Prkdcscid) mice were purchased from Jackson laboratories (Bar Harbor, ME). Mice were injected subcutaneously in each flank with human melanoma cells on day 0. Tumors were measured every 2–3 days with calipers and tumor volume was calculated with the formula $(\text{length} \times \text{width} \times \text{width} \times \pi) / 6$. Mice were sacrificed and tumors were excised and stained by standard immunohistochemistry for CD3 to evaluate T cell infiltration.

CONFLICT OF INTEREST

The authors declare no conflict of interest.

ACKNOWLEDGMENTS

The authors thank the MSKCC antitumor assessment and cytology cores at MSKCC. This research was in part supported by the Cancer Research Institute (MS), the Lake Road Foundation (MS) NIH grant T32CA009512 (MVM), the Ludwig Trust and Swim Across America (SDW) and the MSK core grant NIH P30-CA008748. MS thanks Loyd Old for interesting discussion to initiate this project.

REFERENCES

- Kohn, DB, Dotti, G, Brentjens, R, Savdolo, B, Jensen, M, Cooper, LJ *et al.* (2011). CARs on track in the clinic. *Mol Ther* **19**: 432–438.
- Sadelain, M (2015). CAR therapy: the CD19 paradigm. *J Clin Invest* **125**: 3392–3400.
- Kochenderfer, JN, Wilson, WH, Janik, JE, Dudley, ME, Stetler-Stevenson, M, Feldman, SA *et al.* (2010). Eradication of B-lineage cells and regression of lymphoma in a patient treated with autologous T cells genetically engineered to recognize CD19. *Blood* **116**: 4099–4102.
- Kalos, M, Levine, BL, Porter, DL, Katz, S, Grupp, SA, Bagg, A *et al.* (2011). T cells with chimeric antigen receptors have potent antitumor effects and can establish memory in patients with advanced leukemia. *Sci Transl Med* **3**: 95ra73.
- Brentjens, RJ, Davila, ML, Riviere, I, Park, J, Wang, X, Cowell, LG *et al.* (2013). CD19-targeted T cells rapidly induce molecular remissions in adults with chemotherapy-refractory acute lymphoblastic leukemia. *Sci Transl Med* **5**: 177ra38.
- Hinrichs, CS and Restifo, NP (2013). Reassessing target antigens for adoptive T-cell therapy. *Nat Biotechnol* **31**: 999–1008.
- Morello, A, Sadelain, M and Adusumilli, PS (2016). Mesothelin-targeted CARs: driving T cells to solid tumors. *Cancer Discov* **6**: 133–146.
- Cheever, MA, Allison, JP, Ferris, AS, Finn, OJ, Hastings, BM, Hecht, TT *et al.* (2009). The prioritization of cancer antigens: a national cancer institute pilot project for the acceleration of translational research. *Clin Cancer Res* **15**: 5323–5337.
- Bendle, GM, Linnemann, C, Hooijkaas, AI, Bies, L, de Witte, MA, Jorritsma, A *et al.* (2010). Lethal graft-versus-host disease in mouse models of T cell receptor gene therapy. *Nat Med* **16**: 565–571.
- Brenner, M (2010). T cell receptors and cancer: gain gives pain. *Nat Med* **16**: 520–521.
- Robbins, PF, Morgan, RA, Feldman, SA, Yang, JC, Sherry, RM, Dudley, ME *et al.* (2011). Tumor regression in patients with metastatic synovial cell sarcoma and melanoma using genetically engineered lymphocytes reactive with NY-ESO-1. *J Clin Oncol* **29**: 917–924.
- Rapoport, AP, Stadtmauer, EA, Binder-Scholl, GK, Golubeva, O, Vogl, DT, Lacey, SF *et al.* (2015). NY-ESO-1-specific TCR-engineered T cells mediate sustained antigen-specific antitumor effects in myeloma. *Nat Med* **21**: 914–921.
- Stone, JD, Harris, DT, Soto, CM, Chervin, AS, Aggen, DH, Roy, EJ *et al.* (2014). A novel T cell receptor single-chain signaling complex mediates antigen-specific T cell activity and tumor control. *Cancer Immunol Immunother* **63**: 1163–1176.
- Greenspan, NS (2001). Affinity, complementarity, cooperativity, and specificity in antibody recognition. *Curr Top Microbiol Immunol* **260**: 65–85.
- van der Stegen, SJ, Hamieh, M and Sadelain, M (2015). The pharmacology of second-generation chimeric antigen receptors. *Nat Rev Drug Discov* **14**: 499–509.
- Denkberg, G and Reiter, Y (2006). Recombinant antibodies with T-cell receptor-like specificity: novel tools to study MHC class I presentation. *Autoimmun Rev* **5**: 252–257.
- Hülsmeier, M, Chames, P, Hillig, RC, Stanfield, RL, Held, G, Coulie, PG *et al.* (2005). A major histocompatibility complex-peptide-restricted antibody and T cell receptor molecules recognize their target by distinct binding modes: crystal structure of human leukocyte antigen (HLA)-A1-MAGE-A1 in complex with FAB-HYB3. *J Biol Chem* **280**: 2972–2980.
- Stewart Jones, G *et al.* (2009). Rational development of high-affinity T-cell receptor-like antibodies. *Proc Natl Acad Sci USA* **106**: 5784–5788.
- Gnjatic, S, Nishikawa, H, Jungbluth, AA, Güre, AO, Ritter, G, Jäger, E *et al.* (2006). NY-ESO-1: review of an immunogenic tumor antigen. *Adv Cancer Res* **95**: 1–30.
- Maher, J, Brentjens, RJ, Gunset, G, Riviere, I and Sadelain, M (2002). Human T-lymphocyte cytotoxicity and proliferation directed by a single chimeric TCR ζ /CD28 receptor. *Nat Biotechnol* **20**: 70–75.
- Holler, PD, Chlewicki, LK and Kranz, DM (2003). TCRs with high affinity for foreign pMHC show self-reactivity. *Nat Immunol* **4**: 55–62.
- Weber, KS, Donermeyer, DL, Allen, PM and Kranz, DM (2005). Class II-restricted T cell receptor engineered *in vitro* for higher affinity retains peptide specificity and function. *Proc Natl Acad Sci USA* **102**: 19033–19038.
- Colf, LA, Bankovich, AJ, Hanick, NA, Bowerman, NA, Jones, LL, Kranz, DM *et al.* (2007). How a single T cell receptor recognizes both self and foreign MHC. *Cell* **129**: 135–146.
- Zhao, Y *et al.* (2007). High affinity TCRs generated by phage display provide CD4+ T cells with the ability to recognize and kill tumor cell lines. *J Immunol* **179**: 5845–5854.
- Li, Y *et al.* (2005). Directed evolution of human T-cell receptors with picomolar affinities by phage display. *Nat Biotechnol* **23**: 349–354.
- Cole, DK, Pumphrey, NJ, Boulter, JM, Sami, M, Bell, JI, Gostick, E *et al.* (2007). Human TCR-binding affinity is governed by MHC class restriction. *J Immunol* **178**: 5727–5734.
- Chen, JL, Stewart-Jones, G, Bossi, G, Lissin, NM, Wooldridge, L, Choi, EM *et al.* (2005). Structural and kinetic basis for heightened immunogenicity of T cell vaccines. *J Exp Med* **201**: 1243–1255.
- Latouche, JB and Sadelain, M (2000). Induction of human cytotoxic T lymphocytes by artificial antigen-presenting cells. *Nat Biotechnol* **18**: 405–409.
- Shultz, LD, Saito, Y, Najima, Y, Tanaka, S, Ochi, T, Tomizawa, M *et al.* (2010). Generation of functional human T-cell subsets with HLA-restricted immune responses in HLA class I expressing NOD/SCID/IL2r gamma(null) humanized mice. *Proc Natl Acad Sci USA* **107**: 13022–13027.
- Shultz, LD, Lyons, BL, Burzenski, LM, Gott, B, Chen, X, Chaleff, S *et al.* (2005). Human lymphoid and myeloid cell development in NOD/LtSz-scid IL2R gamma null mice engrafted with mobilized human hemopoietic stem cells. *J Immunol* **174**: 6477–6489.
- Milone, MC, Fish, JD, Carpenito, C, Carroll, RG, Binder, GK, Teachey, D *et al.* (2009). Chimeric receptors containing CD137 signal transduction domains mediate enhanced survival of T cells and increased antileukemic efficacy *in vivo*. *Mol Ther* **17**: 1453–1464.
- Markley, JC and Sadelain, M (2010). IL-7 and IL-21 are superior to IL-2 and IL-15 in promoting human T cell-mediated rejection of systemic lymphoma in immunodeficient mice. *Blood* **115**: 3508–3519.
- Tassef, DV, Cheng, M and Cheung, NK (2012). Retargeting NK92 cells using an HLA-A2-restricted, EBNA3C-specific chimeric antigen receptor. *Cancer Gene Ther* **19**: 84–100.
- Zhang, G *et al.* (2014). Anti-melanoma activity of T cells redirected with a TCR-like chimeric antigen receptor. *Sci Rep* **4**: 3571.
- Zhao, Q, Ahmed, M, Tassef, DV, Hasan, A, Kuo, TY, Guo, HF *et al.* (2015). Affinity maturation of T-cell receptor-like antibodies for Wilms tumor 1 peptide greatly enhances therapeutic potential. *Leukemia* **29**: 2238–2247.
- Oren, R, Hod-Marco, M, Haus-Cohen, M, Thomas, S, Blat, D, Duvshani, N *et al.* (2014). Functional comparison of engineered T cells carrying a native TCR versus TCR-like antibody-based chimeric antigen receptors indicates affinity/avidity thresholds. *J Immunol* **193**: 5733–5743.
- Inaguma, Y, Akahori, Y, Murayama, Y, Shiraiishi, K, Tsuzuki-Iba, S, Endoh, A *et al.* (2014). Construction and molecular characterization of a T-cell receptor-like antibody and CAR-T cells specific for minor histocompatibility antigen HA-1H. *Gene Ther* **21**: 575–584.
- Chames, P, Hufton, SE, Coulie, PG, Uchanska-Ziegler, B and Hoogenboom, HR (2000). Direct selection of a human antibody fragment directed against the tumor T-cell epitope HLA-A1-MAGE-A1 from a nonimmunized phage-Fab library. *Proc Natl Acad Sci USA* **97**: 7969–7974.
- König, R (2002). Interactions between MHC molecules and coreceptors of the TCR. *Curr Opin Immunol* **14**: 75–83.
- Schmid, DA, Irving, MB, Posevitz, V, Hebeisen, M, Posevitz-Fejfar, A, Sarria, JC *et al.* (2010). Evidence for a TCR affinity threshold delimiting maximal CD8 T cell function. *J Immunol* **184**: 4936–4946.
- Haso, W, Lee, DW, Shah, NN, Stetler-Stevenson, M, Yuan, CM, Pastan, IH *et al.* (2013). Anti-CD22-chimeric antigen receptors targeting B-cell precursor acute lymphoblastic leukemia. *Blood* **121**: 1165–1174.
- Stephan, MT, Ponomarev, V, Brentjens, RJ, Chang, AH, Dobrenkov, KV, Heller, G *et al.* (2007). T cell-encoded CD80 and 4-1BBL induce auto- and transcostimulation, resulting in potent tumor rejection. *Nat Med* **13**: 1440–1449.
- Zhao, Z, Condomines, M, van der Stegen, SJ, Perna, F, Kloss, CC, Gunset, G *et al.* (2015). Structural design of engineered costimulation determines tumor rejection kinetics and persistence of CART cells. *Cancer Cell* **28**: 415–428.
- Krause, A, Guo, HF, Latouche, JB, Tan, C, Cheung, NK and Sadelain, M (1998). Antigen-dependent CD28 signaling selectively enhances survival and proliferation in genetically modified activated human primary T lymphocytes. *J Exp Med* **188**: 619–626.
- Kloss, CC, Condomines, M, Cartellieri, M, Bachmann, M and Sadelain, M (2013). Combinatorial antigen recognition with balanced signaling promotes selective tumor eradication by engineered T cells. *Nat Biotechnol* **31**: 71–75.
- Zhong, XS, Matsushita, M, Plotkin, J, Riviere, I and Sadelain, M (2010). Chimeric antigen receptors combining 4-1BB and CD28 signaling domains augment PI 3 kinase/AKT/Bcl-X L activation and CD8 T cell-mediated tumor eradication. *Mol Ther* **18**: 413–420.



This work is licensed under a Creative Commons Attribution-NonCommercial-NoDerivs 4.0 International License. The images or other third party material in this article are included in the article's Creative Commons license, unless indicated otherwise in the credit line; if the material is not included under the Creative Commons license, users will need to obtain permission from the license holder to reproduce the material. To view a copy of this license, visit <http://creativecommons.org/licenses/by-nc-nd/4.0/>

© The Author(s) (2016)

Supplementary Information accompanies this paper on the *Molecular Therapy—Oncolytics* website (<http://www.nature.com/mto>)